# Advanced Kalman Filter-based Backstepping Control of AC Microgrids: A Command Filter Approach

Vafamand, Navid; Arefi, Mohammad Mehdi; Anvari-Moghaddam, Amjad

*Published in:*
I E E E Systems Journal

*DOI (link to publication from Publisher):*
10.1109/JSYST.2022.3221522

*Publication date:*
2023

*Document Version*
Accepted author manuscript, peer reviewed version

This article has been accepted for publication in IEEE Systems Journal. This is the author's version which has not been fully edited and content may change prior to final publication. Citation information: DOI 10.1109/JSYST.2022.3221522



# Advanced Kalman Filter-based Backstepping Control of AC Microgrids: A Command Filter Approach

Navid Vafamand, Mohammad Mehdi Arefi, *Senior Member, IEEE*, and Amjad Anvari-Moghaddam, *Senior Member, IEEE*

***Abstract*— The stability of alternating current microgrids (AC MGs) is significantly affected by the procedure of collecting precise and sufficient information of the system and tightly controlling power inverters. Whereas using many sensors increases AC MG ripples and cost, integrating cost-effective and low number of sensors is preferred. Further, assuring the stability and tracking issue of AC MGs in different operating modes and in the presence of unknown time-varying loads is a hard task. Aiming at these issues, this paper proposes an improved augmented-Kalman filter to estimate the state vector and disturbance inputs and a nonlinear backstepping controller with a command filter to design the control law. Compared to the conventional Kalman filters, the developed approach is able to estimate the external disturbances, which improves the state estimation performance and provides extra information about the power system. The proposed command filter-based backstepping has the key feature of avoiding the calculation of time-derivatives of desired references of virtual inputs, which is a common drawback of conventional approaches. Whereas the dynamics of the disturbance time-varying load are not available, the command filter is utilized to avoid the time derivatives terms of the disturbance inputs. Simulation results illustrate the estimation performance of the augmented Kalman filter and the tracking performance of the command filter-based backstepping controller.**

***Keywords*— *AC microgrid (MG), Backstepping controller, Kalman filter, Unknown time-varying load, Command filter.***

## NOMENCLATURE

### A. AC MG system parameters

| | |
|---|---|
| $r_f$, $C_f$, $L_f$ | Filter resistance, capacitance, and inductance |
| $v_{od}$, $v_{oq}$ | Bus voltages in the $dq$ framework |
| $i_{od}$, $i_{oq}$ | Load currents in the $dq$ framework |
| $i_{id}$, $i_{iq}$ | Inverter currents in the $dq$ framework |
| $v_{id}$, $v_{iq}$ | Inverter voltages in the $dq$ framework |
| $\omega$ | AC MG frequency |

### B. Kalman filter parameters

| | |
|---|---|
| $x$ | System state vector |
| $d$ | Parameter vector |
| $x_{KF}$ | Kalman state vector |
| $u$ | Control input vector |
| $A$, $B$, $H$ | Continuous-time system matrices |
| $w_k$, $v_k$ | System and measurement noises |
| $Q_k$, $R_k$ | System and measurement noise covariances |
| $T_s$ | Discretizing constant |
| $\hat{x}_{KF}$ | Estimation of the Kalman state vector |
| $P_{KF}$ | Covariance of the estimation |
| $K_{KF}$ | Kalman gain matrix |

### C. Backstepping controller

| | |
|---|---|
| $x_{1,d}, \ldots, x_{4,d}$ | Desired references for the states |
| $z_1, \ldots, z_4$ | Tracking errors |
| $q_1, \ldots, q_4$ | Command filter states |
| $h_3$, $h_4$ | Virtual control input laws |
| $\gamma_1, \ldots, \gamma_4$ | Control design parameters |

## I. INTRODUCTION

Delivering electricity from the main grid to far consumptions, such as isolated communication stations or remote villages/islands, via transmission lines is technically hard and/or economically inappropriate [1]–[3]. In this regard, an economical solution is supplying power via an islanding mode MG topology, which often includes renewable energy resources (RERs) [4]. In this circumstance, distributed generators (DGs) have the key role of regulating the current, voltage, and maybe the frequency of the MG without any support from the main grid [4], [5]. MGs can be established in the form of AC or direct current (DC) types, solely or jointly [6], [7]. In the AC MGs, the key challenging point is regulating the frequency and voltage of the main bus to supply the load reliably and firmly [4]. It is appropriate that the AC MG control mechanism should deliver sinusoidal output voltages and currents with low total harmonic distortion (THD) [8]–[10], be robust against grid disturbances, and provide fast and effective voltage and frequency regulation. As yet, to achieve such characteristics, different linear and nonlinear control methods have already been recommended in the literature [11], [12]. Some of the linear control approaches are proportional-integral-derivative (PID) [13], robust dynamical state-feedback [14], and internal model principle [15]. Nevertheless, the AC MG

N. Vafamand and M.M. Arefi are with the School of Electrical and Computer Engineering, Shiraz University, Shiraz, Iran (e-mails: {n.vafamand, arefi }@shirazu.ac.ir).

A. Anvari-Moghadam is with the Department of Energy (AAU Energy), Aalborg University, 9220 Aalborg, Denmark (email: aam@energy.aau.dk).

This article has been accepted for publication in IEEE Systems Journal. This is the author's version which has not been fully edited and content may change prior to final publication. Citation information: DOI 10.1109/JSYST.2022.3221522



control action is more of a time-varying and nonlinear system owing to DG uncertainties, unknown load disturbances, switching behaviors of the inverters, and operation mode transitions. Hence, linear control methods are less possible to satisfy the desired performance and control objectives. Thereby, most of the conventional linear control approaches only provide average performance in some limited operating situations. To tackle this issue, nonlinear control methods such as feedback linearization [16], active disturbance rejection [17], state bounds constrained dynamic [18], model predictive [8], and sliding mode [2], [19] are suggested in the literature. Although the above nonlinear methods can theoretically assure the AC MG stability, their control laws are functions of the state vector. Since any estimation mechanism to construct the state vector form the measured output vector is not given in those approaches, their developed controllers necessitate measuring all states. In [20], a model reference adaptive backstepping controller is suggested for voltage mode control of AC MGs. A two-state power system is considered and a state observer is presented. However, the above control approaches require the instantaneous values of the loads' currents and even their time-derivative evolutions. On the other hand, to measure the state vector as well as the system time-varying parameters, several current and voltage sensors must be installed. This is undesirably increases the system complexity and total cost, and degrades the performance owning to the ripple filtering effect of current sensors [21]. Moreover, for unknown time-varying loads, computing their time-derivative evolutions in prior is not trivial. Consequently, it is preferred to I) use sensors as low as possible and instead estimate the other information involved in the controller input; II) avoid the time-derivative of unknown loads in the stability analysis.

One effective way to perform the parameters estimation and reduce the number of sensors is the Kalman filter (KF). Mathematically, the KFs are robust against the stochastic system and measurement white noises [22]. Originally, the Kalman filter was used to estimate the state vector of linear and nonlinear systems. After that, it was extended to the case that system parameters are also estimated in the context of augmented Kalman filter [23], Kalman filter with unknown inputs [24], or a more general class of Kalman filter [25]. The KFs have been used in power system applications, including estimating the arc fault in microgrids [26] and actuator and sensor faults in microgrids [27], the state-of-charge in energy storage systems [28], and primary winding current in power transformers [29]. More specifically, for the MGs, the KFs have been developed to estimate the currents and voltages. For example, in [30], [31], and [32] the state vector of a typical DC MG is estimated by extended-KF and cubature-KF, respectively. In [33], an improved KF is applied to a three-phase AC MG to estimate the currents of the AC MG and unknown load power in DC MGs [31]. However, in [33] and [30], the control issue of MG is not studied. Furthermore, the controller of [31] does not assure the closed-loop stability theoretically and the linear controller of [32] leads to poor performance dealing with external disturbance. On the other hand, in order to deal with unknown disturbance dynamics, the command-filter-based backstepping approach can be utilized [34], [35]. In [36], the command filter backstepping controller is considered for an AC MG connected to photovoltaic cells and energy storage units. However, that approach requires that all states, including those of photovoltaic cells and energy storage units, are measurable, which is not practical. Reviewing the above references illustrate that each issue of state estimation and controller design with known load time-derivatives are considered solely. Almost all of the conventional controllers require that dynamics of the loads are given or they are measured via additional sensors. This confines the applicability of the available methods or increases sensor installation and maintenance costs. Besides, the simultaneous consideration of Kalman filter and advanced controller with the assumption that load dynamics are unknown have not been studied yet, which is the key motivating point of this work. More precisely, since the load and its dynamic are unknown, it is required that the controller design procedure is developed so that the closed-loop stability is guaranteed without the need of the load dynamics.

To sum up, this paper proposes a cost-effective augmented-Kalman filter and command-filter-based backstepping controller for AC MGs. The developed Kalman filter estimates both the states and disturbance vectors, simultaneously from the noisy measured output vector. The estimated information is then utilized in the nonlinear backstepping controller to regulate the AC MG bus voltage. Whereas the dynamics of the load are not known, a command-filter technique is developed to avoid them and assure the closed-loop stability and reference tracking, theoretically. This is the main contribution of the proposed approach over the conventional backstepping controllers, which require the dynamics of loads. Assuming that the dynamics of loads are given prior may spoil the theoretical establishment of closed-loop stability in the conventional backstepping controllers. Besides, the proposed approach is robust against noisy measurements, requires a low number of sensors, and is robust against uncertainties and linear and nonlinear loads. It also offers a low online computational burden and complexity, which makes it practical. Numerical simulations are given to show the efficiency of the proposed approach for system state and disturbance estimation, fast regulation, and high-quality power.

This paper is continued by the following sections. Section II presents the mathematical state-space modeling of the three-phase of an AC MG. Section III studies the concept of joint state and disturbance estimation based on an augmented-Kalman filter. Section IV deals with designing a command-filter-based backstepping controller. In Section V, some discussions on the novelty and advantages of the developed approach of Sections III and IV are given. In Section VI, the proposed approach is used to estimate states and disturbance input and control of the AC MG. The suggested future works besides the related conclusion are also summarized in Section VII.

## II. AC MICROGRID TOPOLOGY AND DYNAMICS

An AC MG involves linear and nonlinear loads, DGs, RERs, and energy storage systems, which are incorporated in Fig. 1. Ignoring the RERs and energy storages of the DC MG side, a typical stand-alone three-phase AC MG can be fed using a tightly regulated DC/AC inverter that connects a DC source to the stand-alone AC MG. For simplicity, a diagram of one leg of the three-phase AC MG is given in Fig. 2. The DC/AC inverter is constructed by anti-parallel IGBTs and diode-based

This article has been accepted for publication in IEEE Systems Journal. This is the author's version which has not been fully edited and content may change prior to final publication. Citation information: DOI 10.1109/JSYST.2022.3221522



bidirectional switches to provide a controllable voltage output $v_i$ from the DC source with $V_{DC}$ voltage level. The AC MG feeds several unknown three-phase loads $R_L$ and $L_L$, which in general can be nonlinear, unbalanced, and time-varying.

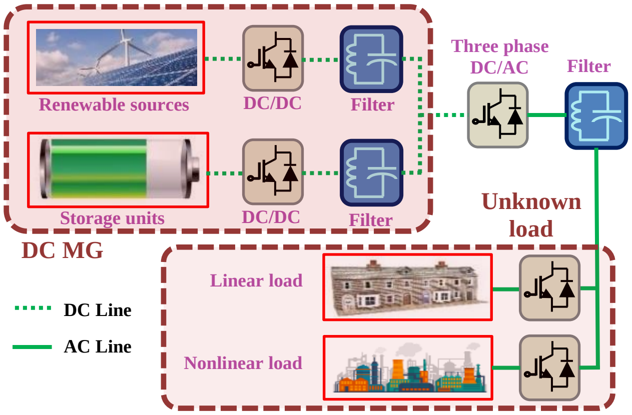


Fig. 1: The diagram of a stand-alone AC MG with different elements.

The dynamics of the stand-alone AC MG of Fig. 2 within the $dq0$ rotating reference frame are obtained as follows [33]:

$$\begin{cases} C_f \dot{v_{od}} = -i_{od} + \omega C_f v_{oq} + i_{id} \\ C_f \dot{v_{oq}} = -i_{oq} - \omega C_f v_{od} + i_{iq} \\ L_f \dot{i_{id}} = -v_{od} - r_f i_{id} + \omega L_f i_{iq} + v_{id} \\ L_f \dot{i_{iq}} = -v_{oq} - r_f i_{iq} - \omega L_f i_{id} + v_{iq} \end{cases} \tag{1}$$

where $i_{od}$ and $i_{oq}$ are the load currents, $i_{id}$ and $i_{iq}$ are the inverter currents, and $v_{od}$ and $v_{oq}$ are the bus voltages. Also, $R_f$, $C_f$, and $L_f$ stand for the resistor, capacitor, and inductor of the RLC filter. By introducing the state vector $x = [x_1\ x_2\ x_3\ x_4]^T = \left[v_{od}\ \ v_{oq}\ \ i_{id}\ \ i_{iq}\right]^T$, and the input vector $u = [u_1\ u_2]^T = \left[v_{id}\ \ v_{iq}\right]^T$, the external disturbance input $d = [d_1\ \ d_2]^T = \left[i_{od}\ \ i_{oq}\right]^T$, the equivalent state-space representation of the dynamics (1) is derived as follows:

$$\begin{cases} \dot{x}_1 = \omega x_2 + 1/C_f x_3 - 1/C_f d_1 \\ \dot{x}_2 = -\omega x_1 + 1/C_f x_4 - 1/C_f d_2 \\ \dot{x}_3 = -1/L_f x_1 - r_f/L_f x_3 + \omega x_4 + 1/L_f u_1 \\ \dot{x}_4 = -1/L_f x_2 - r_f/L_f x_4 - \omega x_3 + 1/L_f u_2 \end{cases} \tag{2}$$

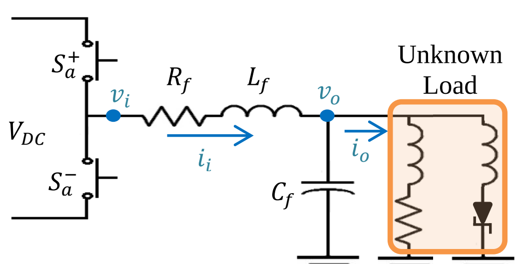


Fig. 2: The diagram of one leg of the stand-alone AC MG.

The objective is to regulate the AC MG bus voltage by using the measured output $y = [y_1\ y_2]^T = [x_1\ x_2]^T$. In (2), the notation external disturbance input for the load currents is used because those terms are not the system states and are unknown. However, the external disturbance inputs can also involve occurring faults, and uncertainties of the RLC filter [2]. The developed controller comprises two parts of the state and disturbance estimation and the command-filter backstepping controller. In the following, these parts will be discussed in detail.

## III. Augmented-Kalman Filter

This section is devoted to extending the conventional Kalman filter to the AC MG with state and disturbance vectors. The developed augmented-Kalman filter should I) estimate the values of the states $x_3$ and $x_4$, II) smooth the noisy values of the states $x_1$ and $x_2$, and III) estimate the external disturbances $d_1$ and $d_2$. To achieve this goal, the disturbance vector $d$ is incorporated with the state vector $x$ to produce an augmented state vector. This idea was originally presented in [37] and has been improved in [23]–[25] as follows:

$$\dot{x}_{KF} = [\dot{x}^T \quad \dot{d}^T]^T \tag{3}$$

whereas the loads' dynamics are unknown in general, one considers that [23]:

$$\dot{d} = 0 \tag{4}$$

Letting $d = [d_1, d_2]^T$ and considering (2)-(4), the augmented state-space model is obtained as follows:

$$\begin{aligned} \dot{x}_{KF} &= A x_{KF} + Bu \\ y &= H x_{KF} \end{aligned} \tag{5}$$

where

$$A = \begin{bmatrix} 0 & \omega & 1/C_f & 0 & -1/C_f & 0 \\ -\omega & 0 & 0 & 1/C_f & 0 & -1/C_f \\ -1/L_f & 0 & -r_f/L_f & \omega & 0 & 0 \\ 0 & -1/L_f & -\omega & -r_f/L_f & 0 & 0 \\ 0 & 0 & 0 & 0 & 0 & 0 \\ 0 & 0 & 0 & 0 & 0 & 0 \end{bmatrix},$$

$$H = \begin{bmatrix} 1 & 0 & 0 & 0 & 0 & 0 \\ 0 & 1 & 0 & 0 & 0 & 0 \end{bmatrix}$$

$$B = \begin{bmatrix} 0 & 0 & 0 & 1/L_f & 0 & 0 \\ 0 & 0 & 1/L_f & 0 & 0 & 0 \end{bmatrix}^T$$

By Applying the forward Euler technique and adding the system and measurement noises $w$ and $v$ to (5), the following discrete state-space model is achieved:

$$\begin{cases} x_{KF,k+1} = (I + T_s A) x_{KF,k} + TBu_k + w_k \\ y_k = H x_{KF} + v_k \end{cases} \tag{6}$$

where white noises $w$ and $v$ shave zero mean and covariance matrices $Q$ and $R$, respectively, $T_s$ stands for the discretizing constant, and the discrete sample number is represented by $k$. The algorithm of the augmented-KF method is as below:

- **Time Update**

$$\begin{aligned} \hat{x}_{KF,k}^- &= \hat{x}_{KF,k-1} + (I + T_s A) x_{KF,k} + TBu_k \\ P_{KF,k}^- &= A P_{KF,k-1} A^T + Q_{k-1} \end{aligned} \tag{7}$$

- **Measurement Update**

$$\begin{aligned} K_{KF,k} &= P_{KF,k}^- H_k^T (H_k P_{KF,k}^- H_k^T + R_k)^{-1} \\ \hat{x}_{KF,k} &= \hat{x}_{KF,k}^- + K_k \left(y_k - H \hat{x}_{KF,k}^-\right) \\ P_{KF,k} &= (I - K_k H_k) P_{KF,k}^- \end{aligned} \tag{8}$$

where $\hat{x}_{KF,k}^-$ and $P_{KF,k}^-$ are predicted states vector and its corresponding predicted covariance matrix ahead of taking into account the system dynamics. Also, involving the measurements in the augmented-KF, the estimated states vector

$\hat{x}_{KF,k}$ and the covariance matrix of the estimated state $P_{KF,k}$ are computed. The filter gain is also expressed by $K_{KF,k}$.

## IV. Backstepping Controller

### A. Command filter approach

The AC MG system contains unknown loads, which can comprise the AC MG loads and/or the grid-connected sharing current. Although the current $i_o$ is estimated by the augmented-Kalman in Section III, its time-derivative is still unknown. To assure closed-loop stability, in this paper, a novel backstepping controller is proposed such that it does not require the time-derivatives of loads. Moreover, to avoid the complex calculation of derivative terms and the need to know the dynamics of the loads, in this paper a command filter approach [34], [35], [38] is developed. By using the command filter in the design procedure, instead of computing their time derivatives, the virtual inputs are filtered by a first-order stable filter and its outputs will be used.

The design procedure of the proposed controller for the AC MG system is decomposed into three parts. The first two parts suggest stabilizing control laws for $u_1$ and $u_2$. In this regard, the state-space representation (2) is split into two strict-feedback forms, where the dynamics of states $x_1$ and $x_2$ possess virtual control input states $x_3$ and $x_4$. Such dynamics can be regulated by the proposed backstepping control method. The simplified strict feedback structure of the dynamics (2) is presented in Fig. 3. As can be seen in Fig. 3, the desired outputs are $x_1$ and $x_2$, which are influenced by the states $x_3$ and $x_4$, respectively. The states $x_3$ and $x_4$ are called virtual inputs for the dynamics $\dot{x}_1$ and $\dot{x}_2$. Therefore, the desired values of the virtual inputs are found so that the outputs track their desired values. After that, the actual control inputs should be designed such that the virtual inputs $x_3$ and $x_4$ reach to their desired value. Finally, the overall stability proof based on the Lyapunov theorem is discussed in the third part.

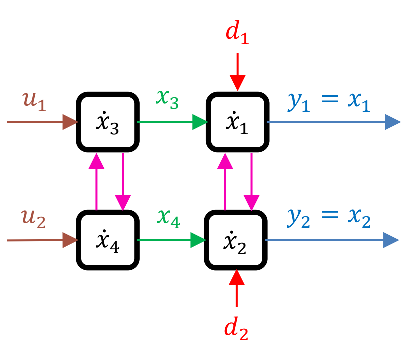


Fig. 3: The AC MG system with the strict feedback form.

### B. Controller design of $u_1 = v_{id}$

Consider that the state $x_1$ tracks the desired differentiable reference $x_{1,d}$. Define the first tracking error as $z_1 = x_1 - x_{1,d} - q_1$ where $q_1$ is updated by

$$\dot{q}_1 = -\gamma_1 q_1 + x_{3,d} - h_3 \quad (9)$$

$$\dot{x_{3,d}} = -\frac{1}{T_{f1}}\left(x_{3,d} - h_3\right) \quad (10)$$

where $\gamma_1 > 0$, $T_{f1}$, and $h_3$ will be defined later. Time derivative of $z_1$ is

$$\dot{z}_1 = \omega x_2 + \frac{1}{C_f}x_3 - \frac{1}{C_f}d_1 - \dot{x}_{1,d} + \gamma_1 q_1 - x_{3,d} + h_3 \quad (11)$$

Defining the third tracking error $z_3 = \frac{1}{C_f}x_3 - x_{3,d} - q_3$ results in

$$\dot{z}_1 = z_3 + q_3 - \frac{1}{C_f}d_1 + \omega x_2 - \dot{x}_{1,d} + \gamma_1 q_1 + h_3 \quad (12)$$

Now, design the virtual control law $h_3$ as follows:

$$h_3 = -\gamma_1\left(x_1 - x_{1,d}\right) - q_3 + \frac{1}{C_f}d_1 - \omega x_2 + \dot{x}_{1,d} \quad (13)$$

Substituting (13) into (12) provides

$$\dot{z}_1 = -\gamma_1 z_1 + z_3 \quad (14)$$

By choosing $\dot{q}_3 = -\gamma_3 q_3$ with $\gamma_3 > 0$, the time derivative of $z_3$ is

$$\dot{z}_3 = -\frac{1}{C_f L_f}x_1 - \frac{r_f}{C_f L_f}x_3 + \frac{\omega}{C_f}x_4 + \frac{1}{C_f L_f}u_1 - \dot{x_{3,d}} + \gamma_3 q_3 \quad (15)$$

The actual control law is designed as follows:

$$u_1 = C_f L_f\left(-\gamma_3\left(\frac{1}{C_f}x_3 - x_{3,d}\right) + \frac{1}{C_f L_f}x_1 + \frac{r_f}{C_f L_f}x_3 - \frac{\omega}{C_f}x_4 + \dot{x_{3,d}} - z_1\right) \quad (16)$$

Substituting (16) into (15) results in

$$\dot{z}_3 = -\gamma_3 z_3 - z_1 \quad (17)$$

### C. Controller design of $u_2 = v_{iq}$

Consider that the state $x_2$ tracks the desired differentiable reference $x_{2,d}$. Let the second tracking error as $z_2 = x_2 - x_{2,d} - q_2$ where $q_2$ is updated by

$$\dot{q}_2 = -\gamma_2 q_2 + x_{4,d} - h_4 \quad (18)$$

$$\dot{x_{4,d}} = -\frac{1}{T_{f2}}\left(x_{4,d} - h_4\right) \quad (19)$$

where $\gamma_2 > 0$, $T_{f2} > 0$, and $h_4$ will be defined later. Time derivative of $z_2$ is

$$\dot{z}_2 = \frac{1}{C_f}x_4 - \frac{1}{C_f}d_2 - \omega x_1 - \dot{x}_{2,d} + \gamma_2 q_2 - x_{4,d} + h_4 \quad (20)$$

Defining the third tracking error $z_4 = \frac{1}{C_f}x_4 - x_{4,d} - q_4$ results in

$$\dot{z}_2 = z_4 + q_4 - \frac{1}{C_f}d_2 - \omega x_1 - \dot{x}_{2,d} + \gamma_2 q_2 + h_4 \quad (21)$$

Now, design the virtual control law $h_4$ as

$$h_4 = -\gamma_2\left(x_2 - x_{2,d}\right) - q_4 + \frac{1}{C}d_2 + \omega x_1 + \dot{x}_{2,d} \quad (22)$$

Substituting (22) into (21) provides

$$\dot{z}_2 = -\gamma_2 z_2 + z_4 \quad (23)$$

By choosing $\dot{q}_4 = -\gamma_4 q_4$ with $\gamma_4 > 0$, the time derivative of $z_4$ is

$$\dot{z}_4 = -\frac{1}{C_f L_f}x_2 - \frac{r_f}{C_f L_f}x_4 - \frac{\omega}{C_f}x_3 + \frac{1}{C_f L_f}u_2 - \dot{x_{4,d}} + \gamma_4 q_4 \quad (24)$$

The actual control law is designed as

$$u_2 = C_f L_f\left(\gamma_4\left(\frac{1}{C_f}x_4 - x_{4,d}\right) + \frac{1}{C_f L_f}x_2 + \frac{r_f}{C_f L_f}x_3 - \frac{\omega}{C_f}x_3 + \dot{x_{4,d}} - z_2\right) \quad (25)$$

This article has been accepted for publication in IEEE Systems Journal. This is the author's version which has not been fully edited and content may change prior to final publication. Citation information: DOI 10.1109/JSYST.2022.3221522



Substituting (16) into (15) results in

$$\dot{z}_4 = -\gamma_4 z_4 - z_2 \tag{26}$$

*D. Stability analysis of the closed-loop system*

In Sub-sections B and C, by substituting the virtual and actual control inputs, the dynamics of the $z_i$ for $i = 1, \ldots, 4$ are obtained. Now, in order to theoretically assure the asymptotic stability of the tracking errors $z_i$, consider a Lyapunov function candidate as follows:

$$V = \frac{1}{2}(z_1^2 + z_2^2 + z_3^2 + z_4^2) \tag{27}$$

The time derivative of (27) along (14), (17), (23), and (26) is equivalent to

$$\dot{V} = -\gamma_1 z_1^2 - \gamma_2 z_2^2 - \gamma_3 z_3^2 - \gamma_4 z_4^2 \tag{28}$$

Now, let $\gamma = \min_{i=1,\ldots,4} \gamma_i$. Thereby, (28) leads into

$$\dot{V} \le -\gamma(z_1^2 + z_2^2 + z_3^2 + z_4^2) = -2\gamma V < 0 \tag{29}$$

Thereby, the exponential stability with the decay rate $\gamma$ [39] is assured.

## V. Contributions and Implementation of the Proposed Controller

**Remark 1 (Comparing the proposed backstepping controller with state-of-the-art methods):** Although several backstepping control approaches have been presented for voltage source control in AC MGs, the conventional backstepping control approach has a common drawback of appearing the time-derivatives of desired references of virtual inputs in the next step of the design procedure. For the VSC of inverters with unknown loads, it is vital to have the time-derivatives of currents of unknown loads and disturbances. Three general backstepping-based methods dealing with the time-derivative terms are presented in the literature.

1. The trivial assumption is that the time derivatives of the currents of unknown loads are given [40]. However, measuring the time-derivative of currents is not cost-effective and increases the effect of noise on the closed-loop control system.
2. The second category considers that the time derivatives terms are zero [41]. This assumption restricts the applicability of the control approach to almost constant and smooth loads. However, if the loads change fast over time, the control system performance degrades.
3. In the third category, conventional backstepping control methods are equipped with robust schemes to avoid the time-derivative terms in their control laws [42]. In [42], a sliding mode-based backstepping controller is suggested which is resilient against mismatched uncertainties and disturbance inputs. That approach assumes that the upper bound of time derivatives of the load currents are given and this value is then used in the switching law of the controller. Though, using the sliding mode controller produces chattered control input law, which mandates a high frequency switching in the PWM signal of the inverters.

In contrast to state-of-the-art backstepping controllers, this paper equips the conventional backstepping controller with the so-called command filter approach. In this approach, instead of using the time derivatives of desired references of virtual inputs, the virtual inputs are subjected to a first-order stable filter to approximately compute their time derivatives. As can be seen in (16) and (25), the only derivative terms are $\dot{x}_{3,d}$ and $\dot{x}_{4,d}$, which are available from two stable first-order filters (10) and (19). Also, the error between the real-value and approximation of the time derivative is compensated in the design procedure to assure the closed-loop stability, theoretically. This is the key benefit of the proposed backstepping controller over the state-of-the-art approaches, which make it robust against unknown time-varying loads. Besides, the proposed approach has the following merits:

1. The proposed approach exponentially stabilizes the AC MG voltage to any desired value. The achieved type of stability is rougher stability than the conventional asymptotic one. Based on the exponential stability, the tracking errors converge to zero with an exponential term push. However, the conventional model predictive methods [6], [31] cannot assure stability theoretically.
2. The developed approach does not need the information of all system states and parameters. whereas the augmented-Kalman filter is developed to estimate the current of the AC MG system, only based on the measured bus voltage. Compared to the conventional Kalman filters [43], [44], the considered augmented Kalman filter can estimate the disturbance input $d = [d_1 \quad d_2]^T = \left[i_{od} \quad i_{oq}\right]^T$ and other states $[x_3 \ \ x_4]^T = \left[i_{id} \quad i_{iq}\right]^T$, simultaneously.

**Remark 2 (Implementation of the overall controller):** The overall closed-loop implementation of the AC MG (1) and the proposed controller is illustrated in Fig. 4. The AC bus voltage subjected to noisy measurement $\tilde{v}_o$ is measured and discretized by a sampler to achieve $\tilde{v}_{o,k}$. Then, the Park's transformation is utilized to derive the system outputs in the $dq0$ framework. The suggested augmented-Kalman filter is utilized. It not only estimates the currents of the filter and unknown loads but also estimates the noisy-less information of the noisy measurements $v_{od,k}$ and $v_{oq,k}$. The output of the augmented-Kalman filter is the $x_{KF,k} = [x_k^T \ \ d_k^T]^T$. The value of the system states and distruabnces are then utilized in the command filter-based backstepping controller to compute the control inputs $v_{id,k}$ and $v_{io,k}$. After that the inverse of the Park's transformation is used to obtain the control input $v_{i,k}$ in original framework. By using the zero-order-hold (ZOH), the continuous-time signal $v_i$ is achieved. Applying the pulse-width modulation (PWM) technique, the switching commands of the three-phase converter are achieved. It is worthy to note that the augmented-Kalman filter is discrete-time; meanwhile, the command filter-based backstepping controller is continuous-time. Since, in practice, digital processors are used to implement the overall controller, it is necessary to design a discrete-time controller based on the sampler and ZOH. Therefore, the command filter-based backstepping controller uses the state information at a discrete-time to compute the control input. For sufficiently small values of discretizing and sampling constant, the performance of the overall controller will not degrade.

The implementation of the augmented-Kalman filter and is given in Sections III and IV. The algorithm of the overall controller in the $dq0$ is given in Algorithm 1.

**Remark 3 (Dealing the KF and backstepping controller with the load dynamics):** The best case for designing an observer-based controller is to develop the observer and

This article has been accepted for publication in IEEE Systems Journal. This is the author's version which has not been fully edited and content may change prior to final publication. Citation information: DOI 10.1109/JSYST.2022.3221522



controller independent of the unknown dynamics of the loads. However, the considered KF requires the dynamics of the load. As it is unknown, a trivial choice is to set it to be zero. On the other hand, the novel backstepping controller does not require the dynamics of the parameters. Also, it is inherently robust against uncertainties and inaccuracy state estimation. Thereby, the assumption of the KF that the load dynamics are zero does not spoil the closed-loop stability, as the estimation error is small and bounded.

**Remark 4 (Applicability of the proposed method to other power systems):** The proposed augmented-KF and backstepping controller of this work can be utilized for other power systems with a given state-space representation. For example, the case study of distributed generators and power-sharing and regulation issues based on droop control [45]. It is only required that the state-space representation should be of the strict-feedback form, as one example is given in Fig. 3.

**Remark 5 (Effects of the controller parameters on the system performance):** The controller design procedure of Algorithm 1 comprises 5 steps of initialization. In these steps, the parameters of the augmented-Kalman filter, backstepping controller, and command filter should be selected.

- For the augmented-KF, $\hat{x}_{KF,0}$ and $P_{KF,0}$ should be chosen based on the values of the power system states. If there is a pre-knowledge about the power system states, the initial condition $\hat{x}_{KF,0}$ can be chosen to be near those of the power system and the error covariance matrix $P_{KF,0}$ can be selected small. However, if there is no pre-knowledge of the power system states, the $\hat{x}_{KF,0}$ and $P_{KF,0}$ should be chosen arbitrarily and large enough, respectively. The matrices $R$ and $Q$ are related to system and measurement noises. If there is not a pre-analysis of the noises (including the accuracy of the state-space model and the precision of the measuring tools), they should be chosen large enough to cover their original value. The discretizing constant $T_s$ should be selected based on the sampling rate and the online computational burden. Generally, smaller values of $T_s$ make the estimation more accurate with the expense of fast processing.
- The backstepping controller and command filter parameters $\gamma_i$ for $i = 1, \ldots, 4$ and $T_{fj}$ for $j = 1,2$ influence the tracking error (i.e. $z_i$ for $i = 1, \ldots, 4$) exponential convergence rate and command filter frequency response, respectively as well as the control input amplitude. Higher values of $\gamma_i$ improve the convergence speed with the expense of increasing the controller input amplitude. Meanwhile, smaller values of $T_{fj}$ improve the command filter frequency with the expense of increasing the control input amplitude.

The above effects should be considered to select appropriate values for the parameters of the controller of Algorithm 1.

## VI. Simulation Results

This section presents the results of the proposed Kalman-based backstepping controller. In the first part, the accuracy and efficiency of the Kalman filter are studied in the $dq0$ framework. Two cases of slow and fast time-varying loads are considered. In the second part, the overall controller is utilized to compensate for the time-varying three-phase load.

### E. Augmented Kalman filter

To evaluate the efficiency of the augmented Kalman filter, two cases are presented. In the former case, the load changes in a stepwise manner, which stands for the case that the loads are (dis)connected (from)to the AC MG. Meanwhile, in the latter case, the load changes smoothly. It is assumed that the switching commands of the inverter are fixed, so that $v_{id} = v_{iq} = 250\,V$. The parameters and initial conditions of the augmented Kalman filter are as follows:

$$\begin{cases} x_{KF,0} = [240 \quad 240 \quad 1.5 \quad 1.5 \quad 2 \quad 2]^T \\ R = 10^4 I; Q = 5 \times 10^{-4} I \end{cases} \tag{30}$$

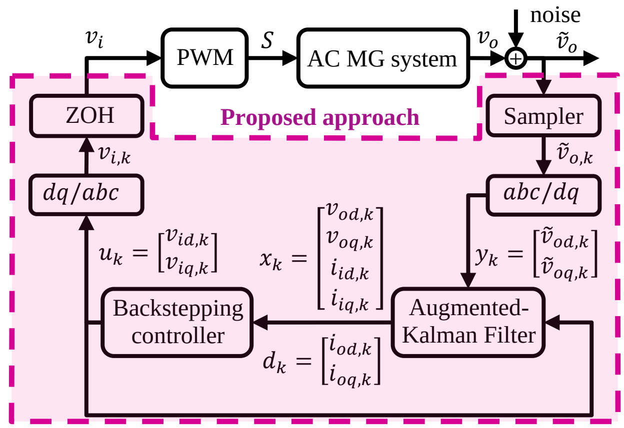

Fig. 4: The closed-loop system implementation.

Algorithm 1: The controller implantation algorithm.

| Action | Description |
|---|---|
| 1. Select the $\hat{x}_{KF,0}$ and $P_{KF,0}$.<br>2. Select the matrices $R$ and $Q$.<br>3. Select discretizing constant $T_s$ | augmented-Kalman filter initialization |
| 4. Select the controller parameters $\gamma_i$ for $i = 1, \ldots, 4$<br>5. Select the command filter parameters $T_{f1}$ and $T_{f2}$. | Controller initialization |
| 6. Remind the control input $u_k$.<br>7. Use the time-update equation (7).<br>8. Measure the system output $y_k$ by a sampler.<br>9. Use the measurement-update equation (8). | Kalman filter implementation to give $x_k$ and $d_k$ |
| 10. Compute $h_3$ and $h_4$ by (14) and (23).<br>11. Use the command filter equation (10) and (19).<br>12. Compute the time-derivatives (11) and (20).<br>13. Compute $u_{1,k}$ and $u_{2,k}$ by (17) and (26). | Controller implementation to give $v_{id,k}$ and $v_{iq,k}$ |
| 14. Apply ZOH on $u_{1,k}$ and $u_{2,k}$ to obtain $v_i$ in.<br>15. Apply dq/abs Transformation to $v_i$.<br>16. Use the PWM block to generate switching signal $S$.<br>17. Apply the switching signal $S$ to the inverter.<br>18. Return to Step 6. | Applying the control input to the three-phase inverter |

Additionally, Table I summarizes the values of the parameters in the AC MG.

Table I. System and load parameters_Sub-section A.

| Parameter | Value | Parameter | Value |
|---|---|---|---|
| $\omega$ | $50\,Hz$ | $C_f$ | $15\,\mu F$ |
| $r_f$ | $0.2\,\Omega$ | $r_{load}$ | $40 \sim 120\,\Omega$ |
| $L_f$ | $2.4\,mH$ | $v_{id}, v_{iq}$ | $250\,V$ |

Figs. 5 and 6 illustrate AC MG states and disturbance load current for the case of stepwise load changes. Since the measured voltages are subjected to noise, in Figs. 5(a)-(b), the noisy measurements, estimated signal, and actual values of the voltages are given. Also, in Figs. 5(c)-(d), the actual and estimated values of current are provided.

This article has been accepted for publication in IEEE Systems Journal. This is the author's version which has not been fully edited and
content may change prior to final publication. Citation information: DOI 10.1109/JSYST.2022.3221522



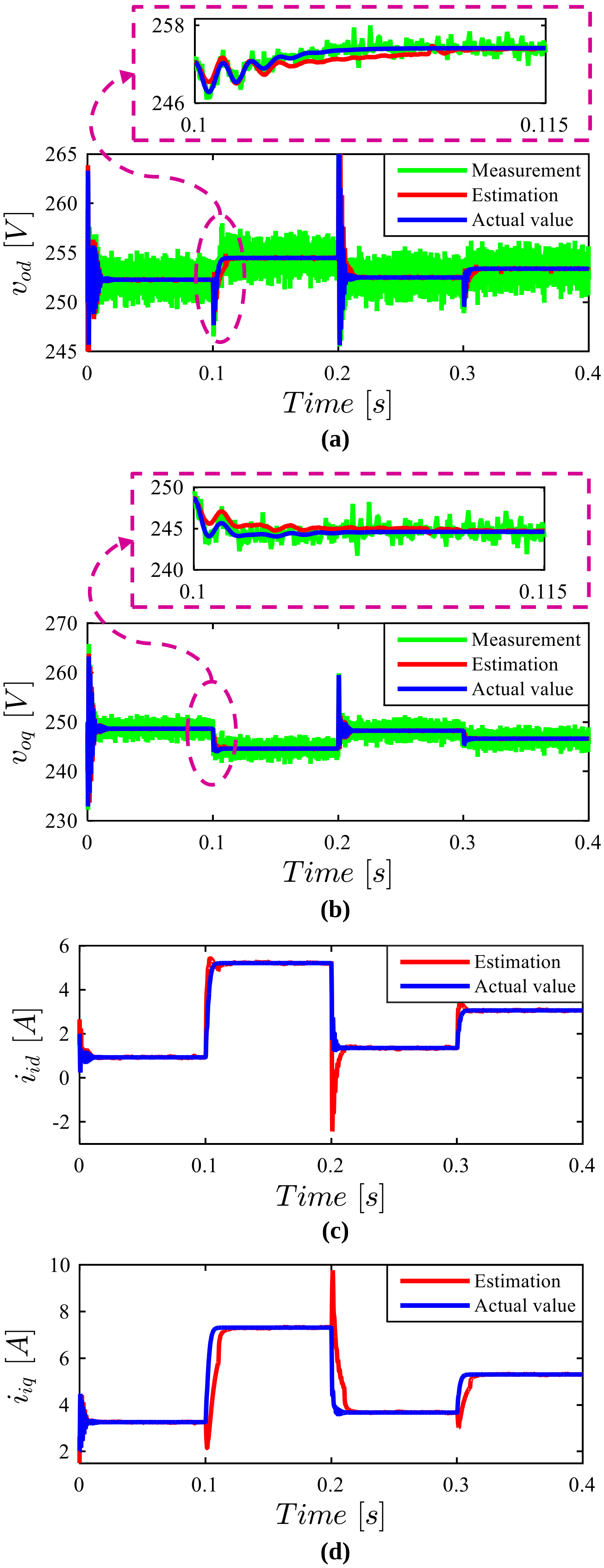


Fig. 5: System state vector $x$_Case 1 (Noisy measured value by the green line, estimated value by the red line, and the actual value by the blue line). **(a).** $x_1 = v_{od}$, **(b).** $x_2 = v_{oq}$, **(c).** $x_3 = i_{id}$, **(d).** $x_4 = i_{iq}$.

From Fig. 5, one infers that the developed augmented Kalman filter reacts to the sudden change of load and the estimated states converge to their actual value in about 0.02 seconds. Also, the proposed approach effectively mitigates the noise effect in the voltage measurements. By comparing the green and red lines, which stand for the noisy measurements and filtered states, it is observed that the augmented-Kalman filter provides a smooth and accurate estimation of voltages. This verifies the robustness of the augmented-KF against noisy measurements. Moreover, in both Figs. 5 and 6, the steady-state estimation error is zero. Fig. 6 reveals that the same transient performance is achieved for estimating the disturbance inputs i.e. (unknown loads currents). More precisely, unknown load currents $d_1 = i_{od}$ and $d_2 = i_{oq}$ change stepwise and the Kalman filter estimates them in about 0.01 seconds.

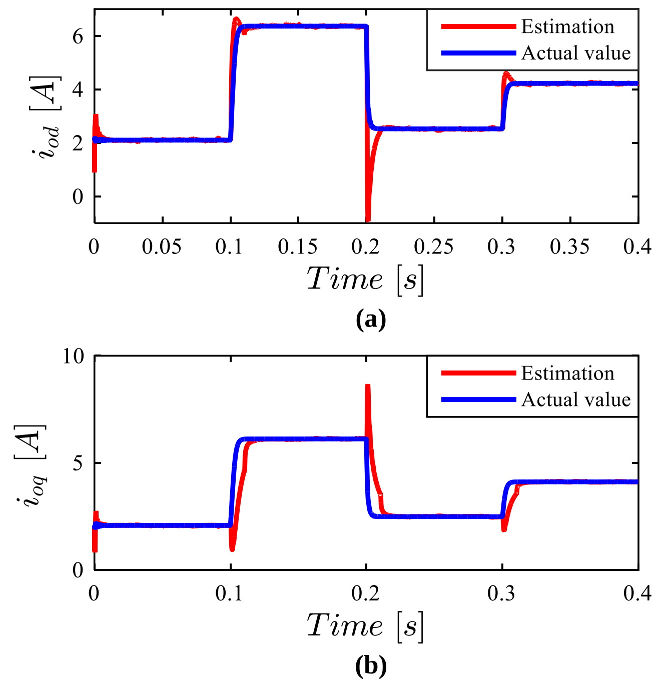


Fig. 6: System disturbance vector $d$ _Case 1 (Estimated value by the red line, and the actual value by the blue line). **(a).** $d_1 = i_{od}$, **(b).** $d_2 = i_{oq}$.

The second case deals with the smooth and slowly varying load change. The same initial condition and parameter as given in (30) are considered. Figs. 7 and 8 depict the actual and estimated values of the states and disturbance.

Figs. 7 and 8 reveal that the augmented-KF estimates slowly varying loads and the states with small and bounded estimation errors. This small estimation error arises from the fact that the estimators have always one step delay in response to the actual value. Fig. 8 indicates that the estimations of disturbance inputs track their corresponding time-varying actual values. However, there is a small delay between the estimation and actual values because the discrete-time Kalman filter initially senses the varying reference and then reacts to it by one step delay.

### *F. Augmented Kalman filter-based Command filter Backstepping controller*

In this sub-section, the stabilizing effect of the proposed approach and its robustness against load variation are evaluated.

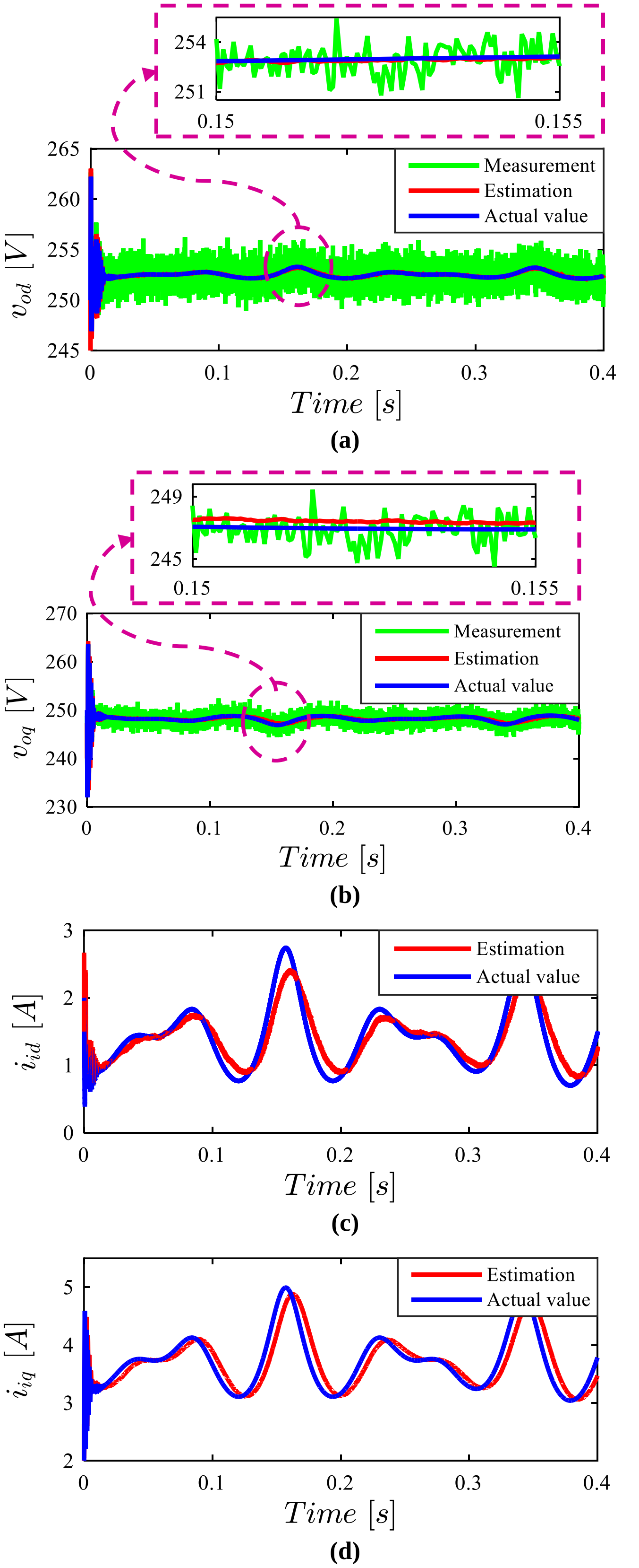


Fig. 7: System state vector $x$_Case 2. (Noisy measured value by the green line, estimated value by the red line, and the actual value by the blue line). **(a).** $x_1 = v_{od}$, **(b).** $x_2 = v_{oq}$, **(c).** $x_3 = i_{id}$, **(d).** $x_4 = i_{iq}$.

The proposed backstepping controller is implemented based on Figs. 3 and 4 with the parameters $\gamma_1 = \gamma_2 = 100$, $\gamma_3 = \gamma_4 = 1000$, $T_{f1} = T_{f2} = 0.0001$. Based on inverse park's transformation and the control laws $u_1 = v_{id}$ and $u_2 = v_{iq}$, the PWM signals for the DC/AC inverter switches are generated. The DC source voltage is fixed at $500\,V$ and the AC MG voltage is supposed to be $V_{o_{rms}} = 200\,V$ for $t \in [0, 0.3]\,sec$ and $V_{o_{rms}} = 100\,V$ for $t \in [0.3, 0.4]\,sec$. Also, a resistive load $r_{load} = 100\,\Omega$ for $t \in [0, 0.1] \cup [0.2, 0.4]\,sec$ and an RL load with $r_{load} = 40\,\Omega$ and $L_{load} = 1\,H$ are considered for $t \in [0.1 \quad 0.2]$. The AC MG parameters are listed in Table II.

Table II: System and load parameter values_Sub-section B.

| Parameter | Value | Parameter | Value |
|---|---|---|---|
| $V_{dc}$ | $500\,V$ | $V_{o_{rms}}$ | $100\sim200\,V$ |
| $r_f$ | $0.2\,\Omega$ | $C_f$ | $15\,\mu F$ |
| $L_f$ | $2.4\,mH$ | $r_{load}$ | $40\sim100\,\Omega$ |
| $L_{load}$ | $1\,H$ | $\omega$ | $50\,Hz$ |

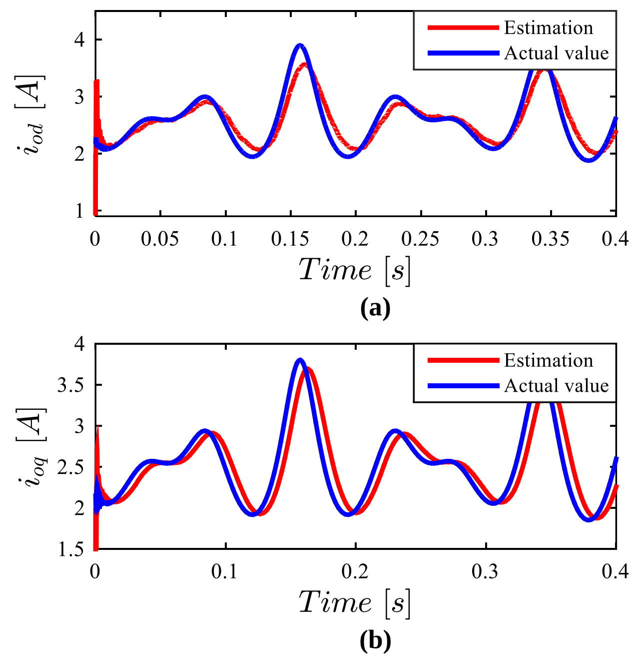


Fig. 8: System disturbance vector $d$_Case 2 (Estimated value by the red line, and the actual value by the blue line). **(a).** $d_1 = i_{od}$, **(b).** $d_2 = i_{oq}$.

Fig. 9 shows the voltages $v_{a,o}$, $v_{b,o}$, and $v_{c,o}$ and the currents $i_{a,o}$, $i_{b,o}$, and $i_{c,o}$ of the AC MG with marks A, B, C, and D. The detail of choosing the marks A, B, C, and D is summarized in Table III.

Table III: The detail of the marks A, B, C, and D in the presence of linear load and desired voltage variation.

| Mark | Detail |
|---|---|
| A | Trainset phase at the start of simulation |
| B | Load changes from 120[Ω] to 80[Ω] |
| C | Load changes from 80[Ω] to 120[Ω] |
| D | Desired voltage changes from 200[V] into 100[$V$] |

Whereas the suggested command filter handles the issue of unknown loads dynamics, the overall controller is robust against the load demand variations, and the voltage is barely affected. At the initial transient phase and the instances of changing the load and the desired reference voltage, AC MG voltage experiences some perturbations and variations as shown in Fig. 9.

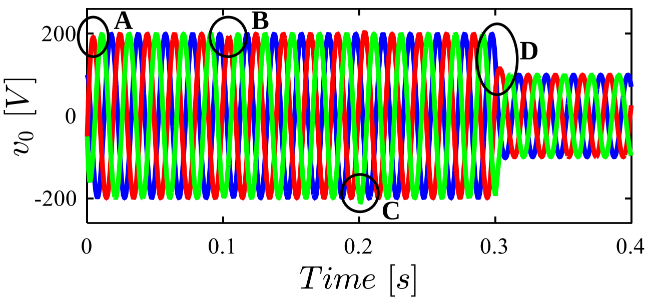


**(a)**

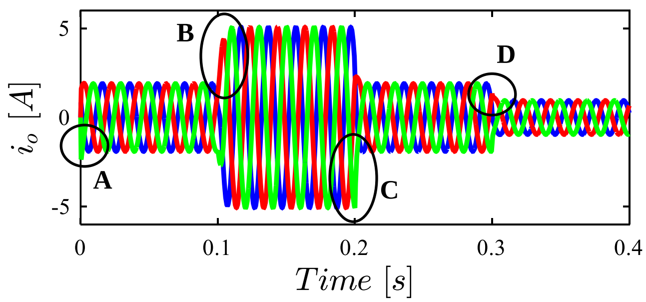


**(b)**

Fig. 9: The voltages and currents of the AC MG- linear load in the abc framework (the blue, red, and green lines stand for the a, b, and c elements of the AC voltage and current, respectively). **(a).** Voltages, **(b).** Currents.

To further challenge the developed approach, it is used to regulate the AC bus voltage in the presence of nonlinear constant power loads (CPLs). The RMS voltage is set as $V_{o_{rms}} = 200\,V$. And a nonlinear load is connected to the AC gird for the time interval $t \in [0.1 \quad 0.3]\,sec$. The bus voltages and load currents achieved by the proposed controller are given in Fig. 10. As can be seen in Fig. 10, the controller acts to unbalanced and time-varying nonlinear load and regulates the bus voltage with small distortion. Also, the proposed approach is compared with [46] and [40]. The reason for choosing those approaches is that they do not use load current sensors same as in this paper. In [46], the controller is designed based on the Jacobian linear matrix of the system and by using the voltage information. In [40], the current of the load is estimated and an adaptive backstepping with the assumption that the time-derivatives of unknown loads are zero is developed.

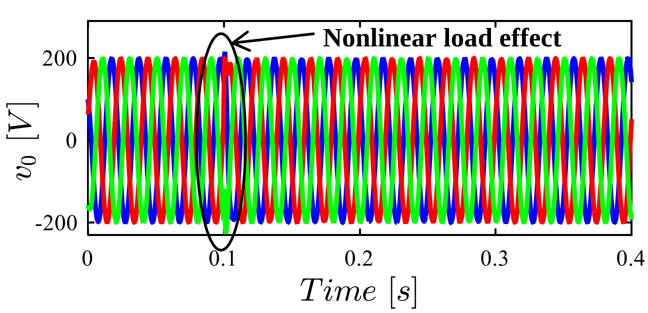


**(a)**

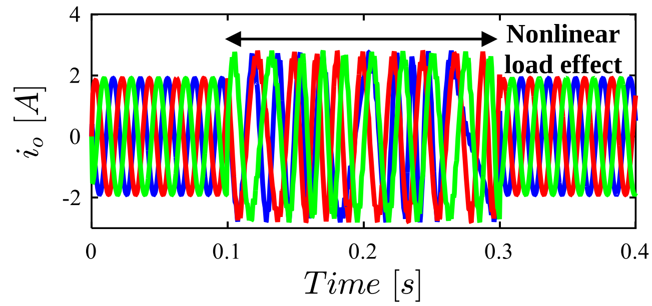


**(b)**

Fig. 10: The voltages and currents of the AC MG- nonlinear load in the abc framework (the blue, red, and green lines stand for the a, b, and c elements of the AC voltage and current, respectively). **(a).** Voltages, **(b).** Currents.

Table IV provides the total harmonic distortion (THD) of the mentioned controllers. The results reveal that the proposed approach outperforms [46] and [40].

Table IV: THD of different controllers in the presence of unbalanced nonlinear load.

| Approach | [46] | [40] | Prop. App. |
|---|---|---|---|
| THD | 1.466% | 1.194% | 0.905% |

## VII. Conclusion

In this paper, a state and disturbance observer-based nonlinear controller was developed to overcome the complexity and heavy computing design of power electronic converters. The filters' and loads' currents in AC MGs are estimated by using an augmented Kalman filter, which is resilient against noisy measurements. Thereby, it avoids installing expensive current sensors. Furthermore, an adaptive robust backstepping controller based on the concept of the command filter backstepping technique was proposed. By deploying the command filter approach, it was theoretically proved that the closed-loop system voltage tracks the reference signal precisely. Simulation results show that the augmented Kalman filter estimates the system states and disturbances for both cases of smooth and prompt variations of loads. Compared to state-of-the-art methods, this approach uses a low number of sensors and theoretically assures the closed-loop system exponential stability. Also, the overall controller is robust against system uncertainties, changes in the value, and type of loads. The presented technique in this paper can be extended as follows: I), other types of estimators such as Luenberger observer or disturbance observer can be utilized. II), Considering the grid-connection operating mode and controlling active and reactive power flows.

## References

[1] A. A. Khodadoost Arani, G. B. Gharehpetian, and M. Abedi, "A Novel Control Method Based on Droop for Cooperation of Flywheel and Battery Energy Storage Systems in Islanded Microgrids," *IEEE Syst. J.*, vol. 14, no. 1, pp. 1080–1087, Mar. 2020, doi: 10.1109/JSYST.2019.2911160.

[2] M. Raeispour, H. Atrianfar, H. R. Baghaee, and G. B. Gharehpetian, "Robust Sliding Mode and Mixed H2/H∞ Output Feedback Primary Control of AC Microgrids," *IEEE Syst. J.*, pp. 1–12, 2020, doi: 10.1109/JSYST.2020.2999553.

[3] A. Navarro-Rodriguez, P. Garcia, R. Georgious, and J. Garcia, "Adaptive Active Power Sharing Techniques for DC and AC Voltage Control in a Hybrid DC/AC Microgrid," *IEEE Trans. Ind. Appl.*, vol. 55, no. 2, pp. 1106–1116, Mar. 2019, doi: 10.1109/TIA.2018.2873543.

[4] N. Vafamand, M. H. Khooban, T. Dragicevic, J. Boudjadar, and M. H. Asemani, "Time-Delayed Stabilizing Secondary Load Frequency Control of Shipboard Microgrids," *IEEE Syst. J.*, pp. 1–9, 2019, doi: 10.1109/JSYST.2019.2892528.

[5] M. Jafari, Z. Malekjamshidi, J. Zhu, and M.-H. Khooban, "Novel Predictive Fuzzy Logic-Based Energy Management System for Grid-connected and Off-grid Operation of Residential Smart Micro-grids," *IEEE J. Emerg. Sel. Top. Power Electron.*, pp. 1–1, 2018, doi: 10.1109/JESTPE.2018.2882509.

[6] N. Vafamand, S. Yousefizadeh, M. H. Khooban, J. D. Bendtsen, and T. Dragicevic, "Adaptive TS Fuzzy-Based MPC for DC Microgrids With Dynamic CPLs: Nonlinear Power Observer Approach," *IEEE Syst. J.*, pp. 1–8, 2018, doi: 10.1109/JSYST.2018.2880135.

[7] N. Vafamand, M. H. Khooban, T. Dragicevic, F. Blaabjerg, and J. Boudjadar, "Robust non-fragile Fuzzy Control of uncertain DC Microgrids Feeding Constant Power Loads," *IEEE Trans. Power Electron.*, pp. 1–1, 2019, doi: 10.1109/TPEL.2019.2896019.

[8] T. Dragicevic, "Model Predictive Control of Power Converters for Robust and Fast Operation of AC Microgrids," *IEEE Trans. Power Electron.*, vol. 33, no. 7, pp. 6304–6317, Jul. 2018, doi: 10.1109/TPEL.2017.2744986.

[9] X. Su, M. Han, J. Guerrero, and H. Sun, "Microgrid Stability Controller Based on Adaptive Robust Total SMC," *Energies*, vol. 8, no. 3, pp. 1784–1801, Mar. 2015, doi: 10.3390/en8031784.

[10] T. Dragicevic and M. Novak, "Weighting Factor Design in Model Predictive Control of Power Electronic Converters: An Artificial Neural Network Approach," *IEEE Trans. Ind. Electron.*, pp. 1–1, 2018, doi: 10.1109/TIE.2018.2875660.

[11] N. Vafamand, M. H. Khooban, T. Dragicevic, and F. Blaabjerg, "Networked Fuzzy Predictive Control of Power Buffers for Dynamic Stabilization of DC Microgrids," *IEEE Trans. Ind. Electron.*, pp. 1–1, 2018, doi: 10.1109/TIE.2018.2826485.

[12] N. Vafamand, M. H. Khooban, T. Dragicevic, F. Blaabjerg, and J. Boudjadar, "Robust non-fragile Fuzzy Control of uncertain DC Microgrids Feeding Constant Power Loads," *IEEE Trans. Power Electron.*, 2019, doi: 10.1109/TPEL.2019.2896019.

[13] N. M. Abdel-Rahim and J. E. Quaicoe, "Analysis and design of a multiple feedback loop control strategy for single-phase voltage-source UPS inverters," *IEEE Trans. Power Electron.*, vol. 11, no. 4, pp. 532–541, Jul. 1996, doi: 10.1109/63.506118.

[14] T. Erfanmanesh and M. Dehghani, "Performance improvement in grid-connected fuel cell power plant: An LPV robust control approach," *Int. J. Electr. Power Energy Syst.*, vol. 67, pp. 306–314, May 2015, doi: 10.1016/j.ijepes.2014.12.006.

[15] N. Pogaku, M. Prodanovic, and T. C. Green, "Modeling, Analysis and Testing of Autonomous Operation of an Inverter-Based Microgrid," *IEEE Trans. Power Electron.*, vol. 22, no. 2, pp. 613–625, Mar. 2007, doi: 10.1109/TPEL.2006.890003.

[16] Dong-Eok Kim and Dong-Choon Lee, "Feedback Linearization Control of Three-Phase UPS Inverter Systems," *IEEE Trans. Ind. Electron.*, vol. 57, no. 3, pp. 963–968, Mar. 2010, doi: 10.1109/TIE.2009.2038404.

[17] R. Errouissi and A. Al-Durra, "A Novel Control Technique for Grid-tied Inverters Considering Unbalanced Grid Voltage Conditions and Control Input Saturation," *IEEE Trans. Sustain. Energy*, pp. 1–1, 2018, doi: 10.1109/TSTE.2018.2883863.

[18] Q.-C. Zhong, G. C. Konstantopoulos, B. Ren, and M. Krstic, "Improved Synchronverters with Bounded Frequency and Voltage for Smart Grid Integration," *IEEE Trans. Smart Grid*, vol. 9, no. 2, pp. 786–796, Mar. 2018, doi: 10.1109/TSG.2016.2565663.

[19] H. R. Baghaee, M. Mirsalim, G. B. Gharehpetian, and H. A. Talebi, "A Decentralized Power Management and Sliding Mode Control Strategy for Hybrid AC/DC Microgrids including Renewable Energy Resources," *IEEE Trans. Ind. Inform.*, pp. 1–1, 2017, doi: 10.1109/TII.2017.2677943.

[20] M. Dehghani *et al.*, "Adaptive backstepping control for master-slave AC microgrid in smart island," *Energy*, vol. 246, p. 123282, May 2022, doi: 10.1016/j.energy.2022.123282.

[21] Q. Xu, C. Zhang, C. Wen, and P. Wang, "A Novel Composite Nonlinear Controller for Stabilization of Constant Power Load in DC Microgrid," *IEEE Trans. Smart Grid*, pp. 1–1, 2018, doi: 10.1109/TSG.2017.2751755.

[22] N. Vafamand, M. M. Arefi, and A. Khayatian, "Nonlinear system identification based on Takagi-Sugeno fuzzy modeling and unscented Kalman filter," *ISA Trans.*, vol. 74, pp. 134–143, Feb. 2018, doi: 10.1016/j.isatra.2018.02.005.

[23] B. Safarinejadian and N. Vafamand, "Kalman Randomized Joint UKF Algorithm for Dual Estimation of States and Parameters in a Nonlinear System," *J. Electr. Eng. Technol.*, vol. 10, no. 3, pp. 1212–1220, May 2015, doi: 10.5370/JEET.2015.10.3.1212.

[24] E. Ghahremani and I. Kamwa, "Local and Wide-Area PMU-Based Decentralized Dynamic State Estimation in Multi-Machine Power Systems," *IEEE Trans. Power Syst.*, vol. 31, no. 1, pp. 547–562, Jan. 2016, doi: 10.1109/TPWRS.2015.2400633.

[25] S. Pan, D. Xiao, S. Xing, S. S. Law, P. Du, and Y. Li, "A general extended Kalman filter for simultaneous estimation of system and unknown inputs," *Eng. Struct.*, vol. 109, pp. 85–98, Feb. 2016, doi: 10.1016/j.engstruct.2015.11.014.

[26] K. Gajula, L. K. Marepalli, X. Yao, and L. Herrera, "Recursive Least Squares and Adaptive Kalman Filter based State and Parameter Estimation for Series Arc Fault Detection on DC Microgrids," *IEEE J. Emerg. Sel. Top. Power Electron.*, pp. 1–1, 2021, doi: 10.1109/JESTPE.2021.3135409.

[27] N. Vafamand, M. M. Arefi, M. H. Asemani, M. S. Javadi, F. Wang, and J. P. S. P. S. Catalao, "Dual-EKF-Based Fault Tolerant Predictive Control of Nonlinear DC Microgrids with Actuator and Sensor Faults," *IEEE Trans. Ind. Appl.*, pp. 1–1, 2022, doi: 10.1109/TIA.2022.3172894.

[28] R. Xiong, H. He, F. Sun, and K. Zhao, "Evaluation on State of Charge Estimation of Batteries With Adaptive Extended Kalman Filter by Experiment Approach," *IEEE Trans. Veh. Technol.*, vol. 62, no. 1, pp. 108–117, Jan. 2013, doi: 10.1109/TVT.2012.2222684.

[29] F. Naseri, Z. Kazemi, M. M. Arefi, and E. Farjah, "Fast Discrimination of Transformer Magnetizing Current From Internal Faults: An Extended Kalman Filter-Based Approach," *IEEE Trans. Power Deliv.*, vol. 33, no. 1, pp. 110–118, Feb. 2018, doi: 10.1109/TPWRD.2017.2695568.

[30] N. Vafamand, S. Yousefizadeh, M. H. Khooban, J. D. Bendtsen, and T. Dragičević, "EKF for Power Estimation of Uncertain Time-Varying CPLs in DC Shipboard MGs," in *IECON 2018-44th Annual Conference of the IEEE Industrial Electronics Society*, 2018, pp. 3413–3418.

[31] S. Yousefizadeh, J. D. Bendtsen, N. Vafamand, M. H. Khooban, T. Dragičević, and F. Blaabjerg, "EKF-based Predictive Stabilization of Shipboard DC Microgrids with Uncertain Time-varying Loads," *J. Emerg. Sel. Top. Power Electron.*, 2018.

[32] M. A. Kardan *et al.*, "Improved Stabilization of Nonlinear DC Microgrids: Cubature Kalman Filter Approach," *IEEE Trans. Ind. Appl.*, vol. 54, no. 5, pp. 5104–5112, Sep. 2018, doi: 10.1109/TIA.2018.2848959.

[33] N. Vafamand, M. M. Arefi, M. S. Javadi, A. Anvari-Moghadam, and J. P. S. Catalao, "Advanced Kalman Filter for Current Estimation in AC Microgrids," in *2020 IEEE International Conference on Environment and Electrical Engineering and 2020 IEEE Industrial and Commercial Power Systems Europe (EEEIC / I&CPS Europe)*, Madrid, Spain, Jun. 2020, pp. 1–6. doi: 10.1109/EEEIC/ICPSEurope49358.2020.9160612.

[34] B. Homayoun, M. M. Arefi, and N. Vafamand, "Robust adaptive backstepping tracking control of stochastic nonlinear systems with unknown input saturation: A command filter approach," *Int. J. Robust Nonlinear Control*, vol. 30, no. 8, pp. 3296–3313, May 2020, doi: 10.1002/rnc.4933.

[35] B. Homayoun, M. M. Arefi, N. Vafamand, and S. Yin, "Neuro-adaptive command filter control of stochastic time-delayed nonstrict-feedback systems with unknown input saturation," *J. Frankl. Inst.*, vol. 357, no. 12, pp. 7456–7482, Aug. 2020, doi: 10.1016/j.jfranklin.2020.04.042.

[36] D. Xu, Y. Dai, C. Yang, and X. Yan, "Adaptive fuzzy sliding mode command-filtered backstepping control for islanded PV microgrid with energy storage system," *J. Frankl. Inst.*, vol. 356, no. 4, pp. 1880–1898, Mar. 2019, doi: 10.1016/j.jfranklin.2019.01.012.

[37] D. Simon, *Optimal state estimation: Kalman, H∞ and nonlinear approaches*. Hoboken, N.J: Wiley-Interscience, 2006.

[38] N. Vafamand, "Adaptive Robust Neural Network-Based Backstepping Control of Tethered Satellites with Additive Stochastic Noise," *IEEE Trans. Aerosp. Electron. Syst.*, pp. 1–1, 2020, doi: 10.1109/TAES.2020.2985276.

[39] H. K. Khalil, *Nonlinear systems*, 3rd ed. Upper Saddle River, N.J: Prentice Hall, 2002.

[40] J. He and X. Zhang, "An Ellipse-Optimized Composite Backstepping Control Strategy for a Point-of-Load Inverter Under Load Disturbance in the Shipboard Power System," *IEEE Open J. Power Electron.*, vol. 1, pp. 420–430, 2020, doi: 10.1109/OJPEL.2020.3016942.

[41] H. Delavari and S. Naderian, "Backstepping fractional sliding mode voltage control of an islanded microgrid," *IET Gener. Transm. Distrib.*, vol. 13, no. 12, pp. 2464–2473, Jun. 2019, doi: 10.1049/iet-gtd.2018.5909.

[42] N. Mahdian Dehkordi and V. Nekoukar, "Robust reliable fault tolerant control of islanded microgrids using augmented backstepping control," *IET Gener. Transm. Distrib.*, vol. 14, no. 3, pp. 432–440, Feb. 2020, doi: 10.1049/iet-gtd.2019.1264.

[43] Y. Shi, K. Sun, L. Huang, and Y. Li, "Online Identification of Permanent Magnet Flux Based on Extended Kalman Filter for IPMSM Drive With Position Sensorless Control," *IEEE Trans. Ind. Electron.*, vol. 59, no. 11, pp. 4169–4178, Nov. 2012, doi: 10.1109/TIE.2011.2168792.

[44] M. Barut, R. Demir, E. Zerdali, and R. Inan, "Real-Time Implementation of Bi Input-Extended Kalman Filter-Based Estimator for Speed-Sensorless Control of Induction Motors," *IEEE Trans. Ind. Electron.*, vol. 59, no. 11, pp. 4197–4206, Nov. 2012, doi: 10.1109/TIE.2011.2178209.

[45] Z. Zhang, C. Dou, D. Yue, and B. Zhang, "Predictive Voltage Hierarchical Controller Design for Islanded Microgrids Under Limited Communication," *IEEE Trans. Circuits Syst. Regul. Pap.*, vol. 69, no. 2, pp. 933–945, Feb. 2022, doi: 10.1109/TCSI.2021.3117048.

[46] J. He, C. Chok You, X. Zhang, Z. Li, and Z. Liu, "An Adaptive Dual-Loop Lyapunov-Based Control Scheme for a Single-Phase UPS Inverter," *IEEE Trans. Power Electron.*, vol. 35, no. 9, pp. 8886–8891, Sep. 2020, doi: 10.1109/TPEL.2020.2974548.

**Navid Vafamand** received his B.Sc. degree in electrical engineering and M.Sc. degree in control engineering form Shiraz University of Technology, Iran, in 2012 and 2014, respectively, and Ph. D. in control engineering at Shiraz University, Shiraz, Iran, in 2019. Currently, he serves as a research assistant at Shiraz University. He was a Ph.D. Visiting student with the Department of Energy Technology, Aalborg University, Denmark, from 2017 to 2018. Dr. Vafamand is the co-author of more than 130 international conference and journal papers and two chapter-books and an active reviewer in several journals. He is among the top 2% of scientists in the world based on the Scopus database for the 2020 single year. His main research interests include Takagi-Sugeno (TS) fuzzy systems, linear parameter varying (LPV) models, predictive control, and DC microgrids.

**Mohammad Mehdi Arefi** (M'17–SM'17) was born in 1982. He received the B.Sc. degree from the Department of Electrical Engineering, Shiraz University, Shiraz, Iran, in 2004, and the M.Sc. and Ph.D. degrees from the Electrical Engineering Department, Iran University of Science and Technology, Tehran, Iran, in 2007 and 2011, respectively. He is an Associate Professor with the Department of Power and Control Engineering, School of Electrical and Computer Engineering, Shiraz University. His current research interests include adaptive robust control, nonlinear control, system identification, and control of power systems.

**Amjad Anvari-Moghaddam** (S'10–M'14–SM'17) received the Ph.D. degree (Hons.) from University of Tehran in 2015 in Power Systems Engineering. Currently, he is an Associate Professor and Leader of Intelligent Energy Systems and Flexible Markets (iGRIDS) Research Group at the Department of Energy (AAU Energy), Aalborg University where he is also acting as the Vice-Leader of Power Electronic Control, Reliability and System Optimization (PESYS) and the coordinator of Integrated Energy Systems Laboratory (IES-Lab). He made a Guest Professor stay with Technische Universität München, Germany during November/December of 2021. His research interests include planning, control and operation management of microgrids, renewable/hybrid power systems and integrated energy systems with appropriate market mechanisms. He has (co)authored more than 270 technical articles, 7 books and 17 book chapters in the field. Dr. Anvari-Moghaddam serves as the Associate Editor of several leading journals such as the IEEE TRANSACTIONS ON POWER SYSTEMS, IEEE Access, IEEE Systems Journal, IEEE Open Access Journal of Power and Energy, and IEEE Power Engineering Letters. He is the Vice-Chair of IEEE Denmark and IEEE-PES Danish Chapter and serves as a Technical Committee Member of several IEEE PES/IES/PELS and CIGRE working groups. He was the recipient of 2020 DUO – India Fellowship Award, DANIDA Research Fellowship grant from the Ministry of Foreign Affairs of Denmark in 2018 and 2021, IEEE-CS Outstanding Leadership Award 2018 (Halifax, Nova Scotia, Canada), and the 2017 IEEE-CS Outstanding Service Award (Exeter-UK).